Comparison of head and thorax cadaver and hybrid III responses to a frontal sled deceleration for the validation of a car occupant mathematical model

Philippe Vezin, Karine Bruyere, François Bermond

VEZIN, Philippe, BRUYERE, Karine, BERMOND, François, 2001, Comparison of head and thorax cadaver and hybrid III responses to a frontal sled deceleration for the validation of a car occupant mathematical model, 17th International Technical Conference on the Enhanced Safety of Vehicles (ESV), AMSTERDAM, PAYS-BAS, 2001-06-04, 10 p

COMPARISON OF HEAD AND THORAX CADAVER AND HYBRID III RESPONSES TO A FRONTAL SLED DECELERATION FOR THE VALIDATION OF A CAR OCCUPANT MATHEMATICAL MODEL

Philippe Vezin, Karine Bruyère, François Bermond
INRETS-LBMC Biomechanics and Impact Mechanics Laboratory, France
Paper number ID#: 114

ABSTRACT

The responses of head and thorax of cadaver and Hybrid III were compared using frontal sled tests. Four pairs of tests were conducted at 50km/h. Two types of force-limiting belt were used. Subject instrumentation included head and spinal accelerometers. Following the tests, autopsies were performed. This research provided complementary information concerning human behaviour during sled test. Local differences for the thorax and the head behaviours between the two restraint systems were identified.
Considering new restraint systems, the comparison of behaviours of the cadaver and the dummy indicates that improvements in the thoracic and head dummy responses have to be made. The results of this study will also be used as validation data for the development of a new numerical model of a driver (HUMOS model - HUman MOdel for Safety).

INTRODUCTION

The general objective of the HUMOS European research program was the development of a new finite element model of a seated car occupant, that could be used in numerical simulations of a car crash with a view to predicting injury risk and injury threshold. Several car manufacturers, car suppliers, software engineering companies, public research institutes and universities were involved in this project.
Car safety is as much a concern for car users and car manufacturers, as for legislative authorities and it represents a key parameter for the evaluation of car performances. As an increasing part of car equipment is dedicated to passive safety, in order to limit the consequences of a car accident, the predictability of safety is a crucial element in the car design phase. Up to now, car manufacturers have mainly relied on crash tests, which simulate car accidents with anthropometric dummies placed in real cars. This solution is not satisfactory since the capability of the dummies to reproduce human behaviour and particularly injury description is limited. In order to predict human behaviour during a car crash, simulation tools shall be based on an accurate model of the human body.
The development of such a model requires a deep knowledge of the human geometry, of its constitutive materials and an experimental database is needed for validation purposes. In the HUMOS project the geometry acquisition of a human subject was done by the INRETS-LBA laboratory (Applied Biomechanics Laboratory of Marseille, France). The methodology used, is based on obtaining referenced serial sections from an entire anatomical subject, frozen in a driving position. The meshing of the geometry and the introduction of the law of the constitutive materials in software were carried out by the other HUMOS partners. The objective of the INRETS-LBMC work in the HUMOS program was to give data of the dynamic and kinematic of PMHS (Post Mortem Human subject) during sled tests for the validation of this finite element model.
During the last decade, a great amount of work has been made with the view of characterising the human dynamic behaviour. A number of experiments have been carried out in order to obtain global information on the human behaviour during frontal sled deceleration. Unfortunately, the lack of coherence between the different studies, together with the difficulties encountered to clearly identify and/or reproduce the used boundary conditions, render the exploitation of those results difficult to achieve. The aim of this study was to give complementary information on this purpose.
This paper presents a part of the information collected for the HUMOS project and focus on the response of the human head and thorax in a frontal sled deceleration test compared with Hybrid III dummy response. The INRETS–LBMC laboratory carried out four PMHS tests (H_01 to H_04) and four dummy tests (D_01 to D_04).

METHOD

Equipment

An experimental protocol was set up according to the needs expressed by the HUMOS consortium. The tests were conducted at the INRETS-LBMC laboratory using a sled system designed for the HUMOS Project. The seat geometry was close to those of a standard mid-size car. The feet of the surrogate were fixed on the footrest. The hands were maintained in the natural driver posture in the 10:10

o'clock position**,** with two nylon wires, which were released at the impact with a mechanical opening. The same device was used to maintain the head in a natural position just before the impact. The seat was adjusted at the same position for each test and was independent of the anthropometry. The seat back was tilted at 20 degrees angle (Figure 1).

Figure 1. Rigid seat for the HUMOS sled tests.

The subjects were restrained by separate shoulder and static pelvis belts. The shoulder belt was equipped with a force-limiting system. Energy absorption by the retractor assembly was controlled through a torsion bar and the belt restraint was a standard production retractor system without a pre-tensioning device. The pre-tension was made manually before the crash. The nominal force limit was 6kN for the two first pairs of tests (two PMHS : H_01 and H_02, and two dummies : D_01 and D_02) and 4kN for the two other pairs of tests (H_03 and H_04; D_03 and D_04). The shoulder belt ran over the left clavicle (continental European driver position).

Test Conditions

A catapult was used to simulate impact, where the boundary conditions (initial speed, deceleration law and stopping distance) were well known. A cable winch coupled with an inertia flywheel propelled a rail-guided carriage. A Personal Computer controlled the operation. The carriage was propelled against a concrete wall, and was stopped by a shock-absorbing system composed of polyurethane tubes. The HUMOS consortium decided to carry out the frontal impacts with car deceleration pulse close to the ONU/ECE/R44-03 regulation (Child's restraint regulation). Table 1. illustrates the different experimental test configurations : sled velocity, maximum acceleration and stopping distance.

Table 1.
HUMOS Tests Conditions

Test	Sled Velocity (km/h)	Max. Sled Decel. (g's)	Stopping Distance (mm)
H_01	48.80	-21.23	620
H_02	48.10	-20.74	615
H_03	49.80	-22.82	595
H_04	48.10	-20.41	590
D_01	47.80	-20.21	620
D_02	48.14	-20.35	620
D_03	48.00	-21.59	600
D_04	46.50	-21.14	600

Test Subjects

The tested subjects were four recent unembalmed cadavers aged between 58 and 76 years. They were examined for HIV or other infectious diseases, anatomic abnormalities or signs of very long decubitus. The cadavers were chosen as closely as possible to the 50th percentile human body defined by the HUMOS consortium: height between 171cm and 178cm, weight between 68kg and 83kg and sitting height between 89.7cm and 93.3cm. The anthropometries of the tested subjects are given in the Table 2. In order to simulate living conditions, pulmonary pressurisation was performed prior to testing. The Hybrid III 50th percentile dummy, calibrated following manufacturer's specifications was used for all test conditions before each cadaver test.

Table 2.
Anthropometric Data From HUMOS Sled Tests

	H_01	H_02	H_03	H_04
Age	76	66	58	70
Weight (kg)	45	76	62	76
Height (cm)	169	180	172	177
Sitting Height (mm)	910	940	900	970

Instrumentation

Sled deceleration and restraint belt loads were recorded for all the tests. The Hybrid III dummies were instrumented with triaxis accelerometers at the chest, the pelvis and the centre of gravity of the head. For the cadaver tests, triaxis accelerometers were mounted on the first and the eighth thoracic vertebrae (T1 and T8). A triaxis accelerometer was also mounted on the sacrum. Each component of

acceleration data was filtered with a digital Butterworth filter channel class 60, prior to compute resultant accelerations. INRETS-LBMC had developed a specific helmet, weighing 330gr, equipped with 12 accelerometers allowing the measurement of the acceleration of the head's centre of gravity of PMHS [1]. The same helmet was used for the Hybrid III dummy and the results were validated by comparison with the accelerations recorded with the accelerometers located at the dummy head's centre of gravity. All data were acquired at 10,000 samples/sec.
High-speed cameras (500 frames/second) were used to record the test, one on the side view and one on the top view. Motion analysis was performed in order to give a qualitative description of the dynamics.

Coordinate systems

The sign convention and standard instrumentation used was the SAE J211 convention (March 1995) for all the tests (dummy and cadaver). In the following, the X (or longitudinal) and Z (or vertical) direction means the moving axis of the accelerometer during the crash. The Z-axis is positive downwards and the X-axis is positive in the crash direction. Concerning the head accelerations, the Frankfurt plane defines the X and Y-axis. The line between the centre of gravity and the midpoint of the line connecting the infraorbital notches defines the positive X-axis. The Y-axis is positive towards the right ear. The resultant was calculated from the three components of the acceleration, the transverse (Y) component, generally negligible, was not presented here.

Response Scaling Procedures

Due to the variability in subject geometry and inertial properties, the subject responses were normalised to the standard anthropometry of the 50th percentile male weighing 75kg. The normalisation procedures of Eppinger et al. [2] were used to perform the scaling. The scaling variable based on the subject mass (M) in kg is shown in equation (1.). The accelerations and times can be expressed in terms of initial parameters, denoted with subscript i, and the scaling factor (Equations 2 and 3).

$$\lambda = (75/M_i)^{1/3} \quad (1.)$$

$$A = \frac{A_i}{\lambda} \quad (2.)$$

$$T = \lambda \times T_i \quad (3.)$$

Despite the fact that the force-limiting device produces loads that were independent to the subject mass when it operates. The shoulder belt load were also normalised in time because the time when the load limiting system started depends on the mass and acceleration of the subject. Moreover, longitudinal, vertical and resultant accelerations were presented using the mean values of the tests performed in the same conditions (same restraint system and same type of surrogate).

Injury description

Pre-test radiographies were conducted to identify any existing injuries or anomalies, but also to verify the mounting and the location of instrumentation. Following the tests, a pathologist and an autopsy specialist performed standard autopsies. Examinations of the cadaver's abdomen, viscera, head and neck, spine, and other skeletal elements were performed. The number and the locations of rib fractures were documented. All injuries were coded according to the Abbreviated Injury Scale (AIS 1990, [3]) and the maximum AIS value (MAIS) was determined.

RESULTS

Figure 2. shows the different sled decelerations compared to the R44-03 regulation corridor (bold line). There was only a little test-to-test variation in the deceleration and in the impact velocity (Table 1.).

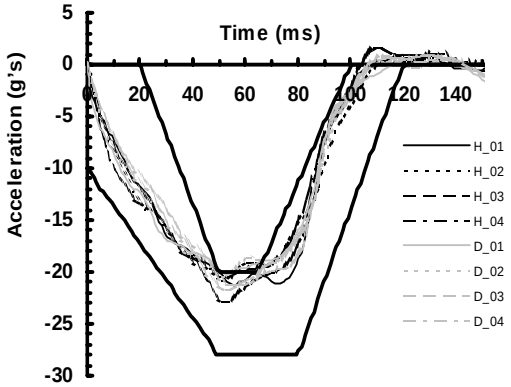

Figure 2. Sled pulse time/history compared with ONU/ECE/R44-03 regulation.

Figures 3.a (6kN load limiting belt) and 3.b (4kN load limiting belt) show the shoulder-belt load versus time for the different tests. It appears that the force-limiting system activates at about 50ms after the beginning of the crash for all the tests. The load begins to fall 50ms after the activation of the force limiting system, as obtained by Shaw and al. [4].

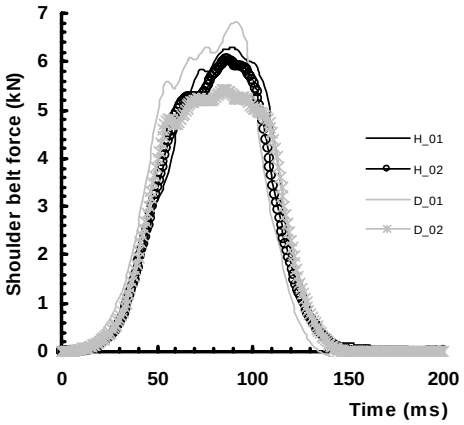

Figure 3.a. Load belt versus time for the 6kN belt.

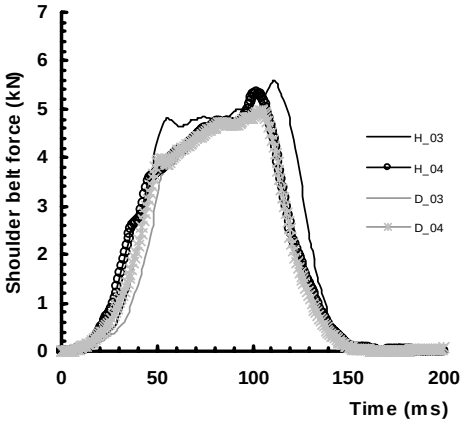

Figure 3.b. Load belt versus time for the 4kN belt.

Pelvis Acceleration

Table 3. summarises the maximal and minimal values of the accelerations measured for the PMHS sacrum and the dummy pelvis.

Table 3.
Maximum Pelvis Acceleration

Test (load limit)	X Min/Max (g's)	Z Min/Max (g's)	Resultant (g's)
H_01 (6kN)	-21.6/12.2	-13.9/4.9	26.4
H_02 (6kN)	-35.4/13.4	-16.0/6.5	35.9
H_03 (4kN)	-24.1/7.1	-19.6/11.4	33.3
H_04 (4kN)	-27.5/14.1	-11.9/7.9	29.9
D_01 (6kN)	-34.2/21.6	-5.9/3.5	35.2
D_02 (6kN)	-37.7/21.4	-9.7/1.9	39.1
D_03 (4kN)	-38.9/19.2	-11.8/5.2	41.1
D_04 (4kN)	-36.7/18.0	-6.6/5.4	37.3

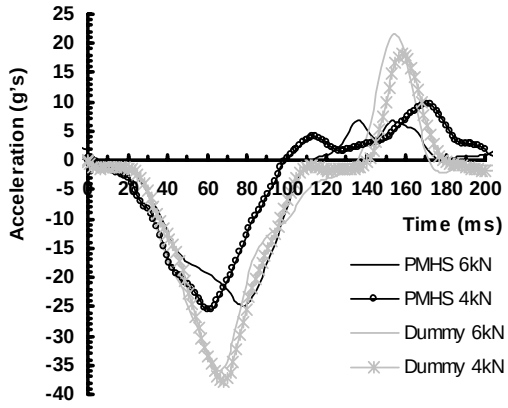

Figure 4. Comparison of the longitudinal pelvis acceleration obtained for different belt load limits.

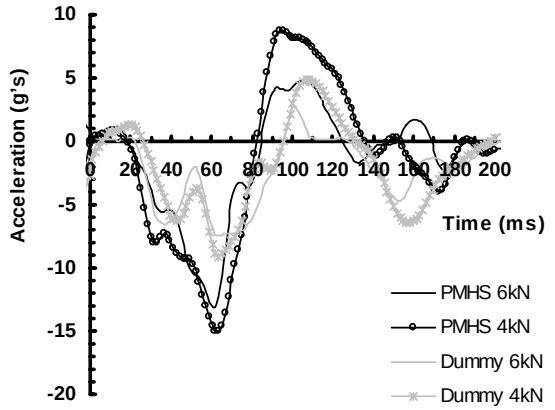

Figure 5. Comparison of the vertical pelvic acceleration obtained for different belt load limits.

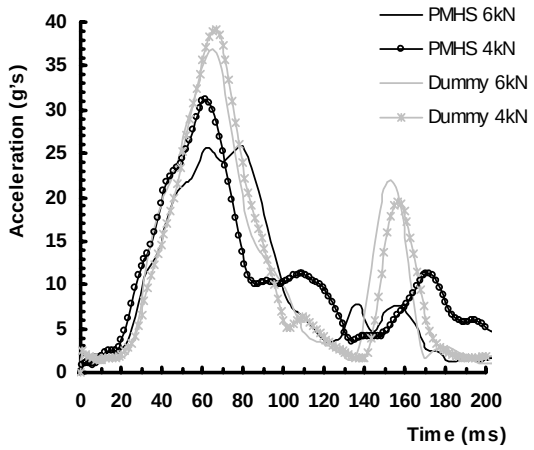

Figure 6. Comparison of resultant pelvic acceleration obtained for different belt load limits.

Time histories are given in Figures 4., 5. and 6. Considering the longitudinal (X) decelerations, values are lower for the PMHS than for the dummy (Figure 4.). It is the contrary for the vertical component, the PMHS accelerations are greater than for the dummy. Regarding the pelvis resultant deceleration, significant difference between the dummy and the cadaver responses has been observed since the dummy deceleration is slightly greater than the PMHS deceleration (Figure 6), without considering the difference of measurement location (on the sacrum for the cadaver and on the pelvis for the dummy). In other words, the global acceleration and the space distribution are different. Due to the greater rigidity of the dummy pelvis.

For the dummy tests, the load limit of the shoulder belt has not a great influence on the dynamics of the pelvis. On the contrary, the change of belt load limit modifies the distribution of the acceleration of the PMHS between the component. The longitudinal deceleration is reduced when though the vertical component increases. The PMHS resultant acceleration is higher with the 4kN belt, it is a consequence of the greater rotation of the thorax due to his lower deceleration (see below).

Thorax Acceleration

The thoracic accelerations of the cadaver are examined with the acceleration of the first (T1) and eighth (T8) vertebrae. The measurement location of chest acceleration on the dummy corresponds approximately to the location of the T8 vertebra acceleration measurement on the cadaver. The maximum accelerations of the PMHS T8 vertebra and the dummy chest are given in the Table 4. Time histories are synthesised in Figures 7. to 9.

Table 4.
Maximum Chest Acceleration

Test (load limit)	X Min/Max (g's)	Z Min/Max (g's)	Resultant (g's)
H_01 (6kN)	-24.5/6.0	NA	NA
H_02 (6kN)	-34.7/6.6	-12.1/6.2	34.8
H_03 (4kN)	-16.4/4.9	-9.1/13.7	16.5
H_04 (4kN)	-21.6/2.8	-9.7/14.6	21.7
D_01 (6kN)	-24.2/2.8	-9.5/12.5	25.8
D_02 (6kN)	-26.3/2.9	-8.0/10.6	27.7
D_03 (4kN)	-22.3/0.2	-10.8/16.4	18.7
D_04 (4kN)	-19.0/0.2	-10.3/15.4	19.2

Response with respect to the value of load-limiting system shows a reduction of the longitudinal deceleration with smaller belt load. Due to the longer elongation of the 4kN load-limiting belt, the subject is less restrained and its deceleration is lower. Even if the effects of the change in the belt load appear clearly for both surrogates. The decreasing of the chest longitudinal deceleration is more important for PMHS than for Hybrid III. This result is correlated with the observation made on the pelvis. Considering the longitudinal acceleration of chest, the difference between the dummy and the cadaver behaviour is not so significant than for the pelvis. In return, the comparison of the vertical acceleration of chest shows a difference between PMHS and Hybrid III behaviour. A time delay between surrogates is observed for the vertical component. The peak value for the dummy is reached about 20ms before that the PMHS attains his maximal value. Considering the resultant linear acceleration of the chest, any obvious difference between the dummy and cadaver behaviours has been showed (Figure 9).

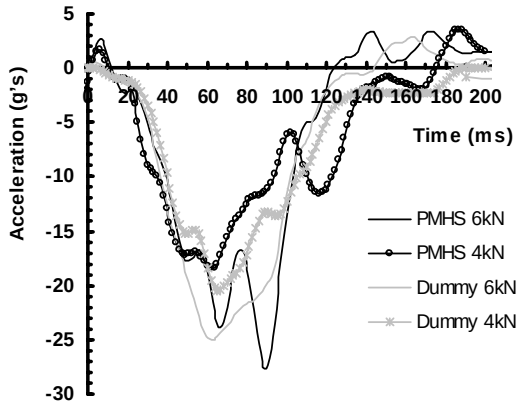

Figure 7. Comparison of the chest longitudinal acceleration obtained for different belt load limits.

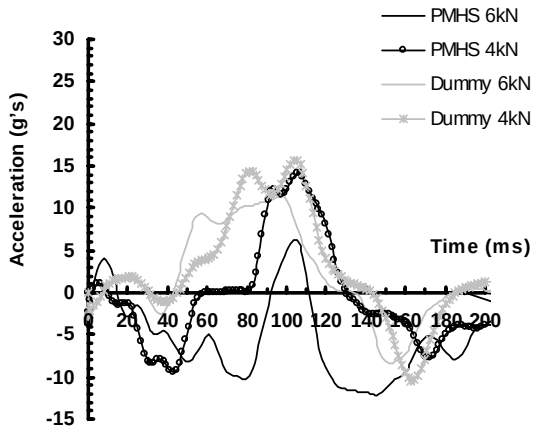

Figure 8. Comparison of the chest vertical acceleration obtained for different belt load limits.

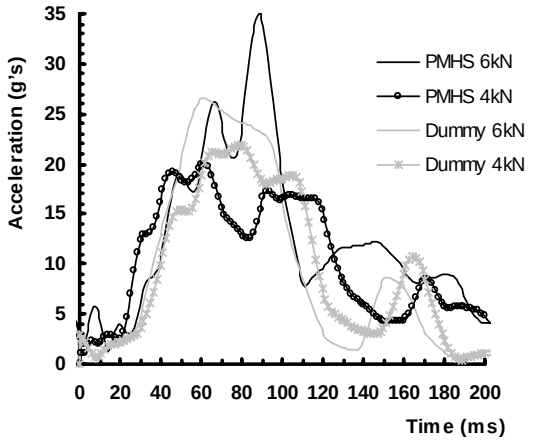

Figure 9. Comparison of the chest resultant acceleration obtained for different belt load limits.

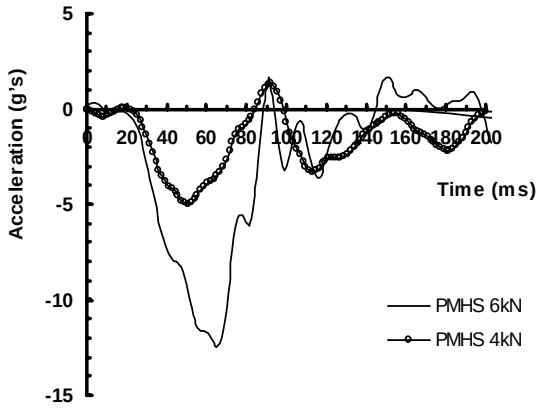

Figure 10. Comparison of the T1 longitudinal acceleration obtained for different belt load limits.

The maximum accelerations of the T1 vertebra for the PMHS tests are summarised in Table 5.

Table 5.
Maximum Accelerations Of T1 Vertebra

Test (load limit)	X Min/Max (g's)	Z Min/Max (g's)	Resultant (g's)
H_01 (6kN)	-13.2/5.1	-5.8/18.5	20.4
H_02 (6kN)	-12.8/8.5	-6.4/26.6	27.5
H_03 (4kN)	-2.9/3.4	-3.2/23.6	23.6
H_04 (4kN)	-8.7/0.1	-4.2/23.0	23.1

The decreasing of the longitudinal deceleration with the diminution of the shoulder belt load described in the former paragraph for T8 is also observed for T1 (Figures 10 to 12). In accordance with the greater displacement in the crash direction, the reduction of the longitudinal component associated to a little increasing of the vertical component could be explain also by a greater rotation around the transverse direction (Y-axis). The change of the orientation of the local axis modified the distribution of the global acceleration between the components. That appears clearly on the side view camera (not shown here).
The top view camera shows a greater rotation of the chest with the higher value of the load shoulder belt for cadaver tests. This rotation around the shoulder belt can explain the difference in the rib fracture locations observed on PMHS and described after. Due to the rigidity of the thorax of the dummy, this observation is not visible on the dummy behaviour. The Hybrid III does not reflect the movement of the clavicle and shoulder articulations.

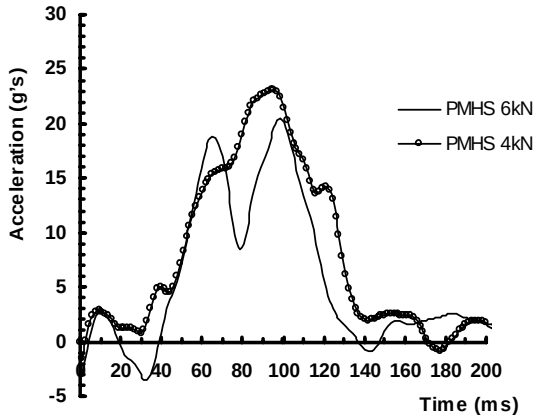

Figure 11. Comparison of the T1 vertical acceleration obtained for different belt load limits.

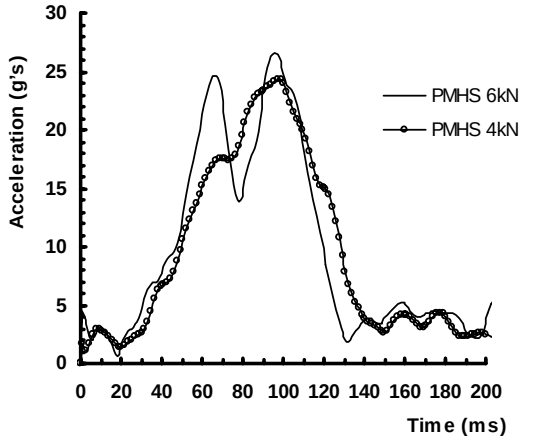

Figure 12. Comparison of the T1 resultant acceleration obtained for different belt load limits.

Head Acceleration

The INRETS-LBMC Laboratory has developed software [1] to calculate the acceleration of the centre of gravity of the head during test on cadaver. This software uses the data from twelve channels of the INRETS-LBMC helmet to compute the acceleration, velocity and displacement components at the centre of gravity of the head and the Head Injury Criterion (HIC at 35ms, Equation 5.).

$$HIC = \left(\frac{1}{t_2 - t_1} \int_{t_1}^{t_2} \gamma(t) dt \right)^{2.5} (t_2 - t_1) \quad (5.)$$

The maximum accelerations and HIC values are collected in Table 6. And time histories on Figures 14. to 16.

Table 6.
Maximum Head Accelerations And HIC

Test (load limit)	X Min/Max (g's)	Z Min/Max (g's)	Resultant (g's)
H_01 (6kN)	-22.9/0.7	-1.5/61.3	65.4
H_02 (6kN)	-27.6/0.4	-2.3/40.0	44.4
H_03 (4kN)	-14.0/0.6	-1.5/25.5	27.5
H_04 (4kN)	-18.3/1.1	-2.7/30.8	32.9
D_01 (6kN)	-24.9/3.5	-2.8/50.8	56.0
D_02 (6kN)	-19.0/9.1	-3.1/57.3	59.6
D_03 (4kN)	-18.0/2.4	-3.4/62.1	56.1
D_04 (4kN)	-17.3/1.3	-2.6/41.6	44.9
Test (load limit)	HIC	Test (load limit)	HIC
H_01 (6kN)	503.4	D_01 (6kN)	490.6
H_02 (6kN)	356.0	D_02 (6kN)	637.6
H_03 (4kN)	171.3	D_03 (4kN)	477.1
H_04 (4kN)	173.8	D_04 (4kN)	350.3

The dummy vertical and resultant head accelerations appear higher than those obtained for the cadavers for all test configurations. It is the contrary for the longitudinal acceleration. This difference increases for the lower belt load value.

It appears that the components and the resultant of the head acceleration are perceptibly reduced with a 4kN load-limiting belt for the both surrogates. However it seems that these changes in the response are less obvious for the dummy than for the PMHS. This difference of behaviour is certainly due to the dynamic of the neck which is not the same. The value of the Head Injury Criterion is also considerably reduced with the 4kN belt.

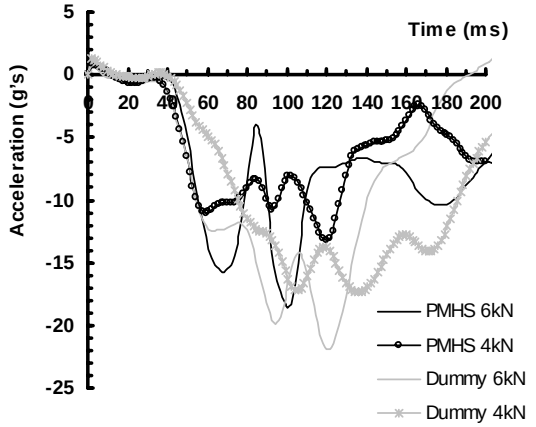

Figure 14. Comparison of the head longitudinal acceleration obtained for different belt load limits.

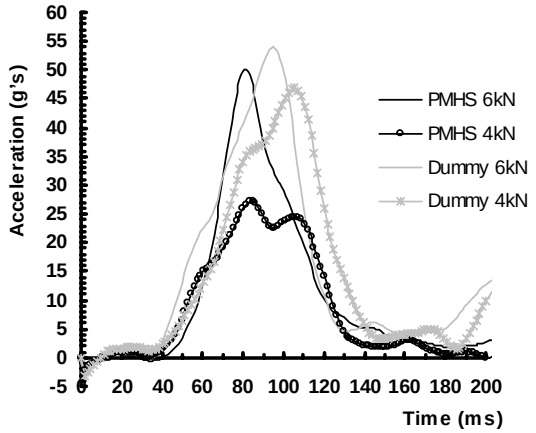

Figure 15. Comparison of the head vertical acceleration obtained for different belt load limits.

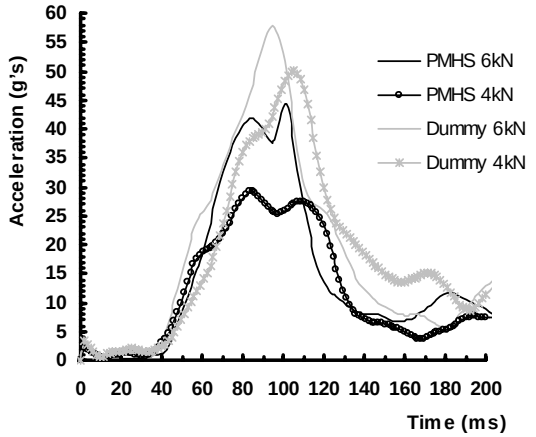

Figure 16. Comparison of the head resultant acceleration obtained for different belt load limits.

Injury Information

No head or neck injuries were identified. The thoracic injuries concerned the ribs, clavicle and sternum. Table 7 summarises the location and the numbers of rib fractures. The locations of the rib fractures are drawn schematically on the Figure 17. It roughly coincides with the line of the belt onto the cadaver's chest. For the tests with a load limit of 6kN, the thorax was massively injured and the number of fractured ribs was considerably reduced with the 4kN load-limiting system. No other injuries were found for all the tests. Table 7. shows the number of fractures for each rib fractured. Table 8. Summarises the number of fractures and the number of fractured ribs for each side of the thorax.

Table 7.
Injury Summary Table, (Rib number $^{\text{fracture number}}$)

Test	Left ribs fractured	Right ribs fractured	Sternal fracture	Clavicle fracture
H_01 (6kN)	2^2, 3^2	1, 2^2, 3^3, 4^3, 5^3, 6^4, 7^2, 8^2, 9^2	yes	yes
H_02 (6kN)	1, 2^2, 3^2, 4, 5, 6, 7	2^2, 3^2, 4^2, 5^2, 6^2, 7^2, 8, 9, 10	yes	yes
H_03 (4kN)	2^4, 3^4, 4^4, 5^3, 6^2, 7	4, 5	no	no
H_04 (4kN)	1, 2^2, 3^2, 4^2, 5,	6	no	no

Table 8.
Number Of Fractures And Fractured Ribs

Test	Number of fractured ribs			Number of fractures		
	Left	Right	Total	Left	Right	Total
H_01 (6kN)	2	9	11	4	22	26
H_02 (6kN)	7	9	16	9	15	24
H_03 (4kN)	6	2	8	18	2	20
H_04 (4kN)	5	1	6	8	1	9

For all test conditions, the left ribs are fractured more often (Table 8). When the shoulder belt load was reduced, the number of fractured ribs on the right side decreased. These results could be correlated with the film analysis, the torso rotation for the PMHS as for dummy is greater for the higher load limit. This rotation could explain the numerous fractures on the right side due to a greater loading on the right side of the thorax. After the tests using the 6kN load limited system, clavicles and sternal fractures were also observed. No fractures were observed on clavicle or sternum with the 4kN load limited belt.

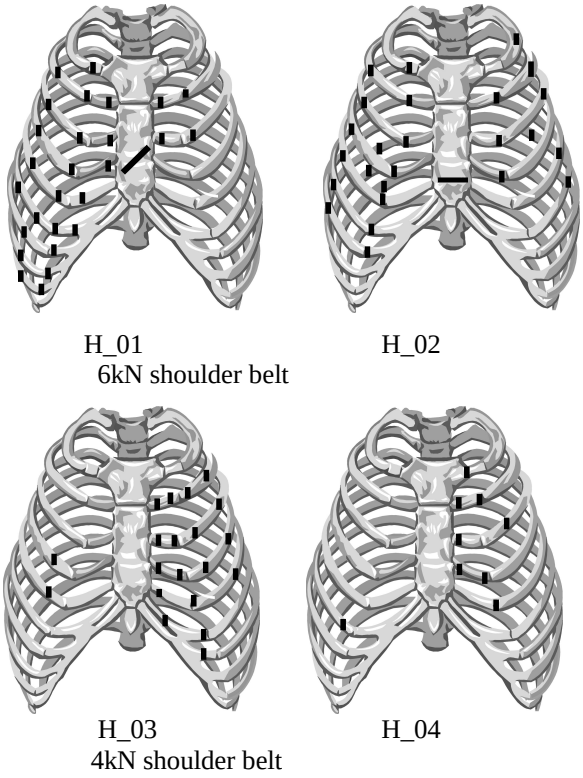

Figure 17. : Rib fracture locations.

The number of fractures is important despite the reduction of the load on the thorax. It is not surprising if we keep in mind the great severity of the impact and the fact that the 4kN shoulder belt is designed to operate with an airbag. A sled test in the same condition with an airbag and a 4kN-shoulder belt has been made in the laboratory and only three fractures were recorded.
The following table gives the AIS and MAIS code for the injured parts. Whatever the load limit, the AIS values were high.

Table 9.
AIS Summary Table

Test	AIS Thorax	AIS Sternum	AIS Clavicle	MAIS
H_01 (6kN)	5	2	2	5
H_02 (6kN)	5	2	2	5
H_03 (4kN)	5	0	0	5
H_04 (4kN)	4	0	0	4

DISCUSSION

This study aimed to provide new data concerning human behaviour during sled tests. In order to use these data for the validation of a numerical model of the human body, the test configuration was simplified, compared to a real car crash situation. The seat was rigid and its position and orientation were the same for each test independently of the anthropometry of the subject. Moreover, the pelvis and shoulder belts were separated. Thus, the influence of the configuration parameters was limited to the effect of the load limit of the shoulder belt.

Caution in applying results obtained with PMHS to living persons is necessary, namely due to the lack of muscle tone in PMHS. However, "the lack of muscle tone is not a serious drawback because muscular response usually occurs too late to affect body kinematics in a crash" as King and Viano wrote [5]. Moreover, variability in the PMHS behaviour can not be avoided due to many parameters such as anthropometry and properties of the biological tissues. In order to limit this variability, subjects were selected as closely as possible to a 50^{th} percentile anthropometry and the PMHS results were normalised.
Considering the difficulties in studying human behaviour, the results presented in this paper allowed us to compare the Hybrid III and PMHS behaviours in a particular loading case and to assess the influence of the load limit of the shoulder belt.

The differences observed in this study, between the dummy and the cadaver behaviours, clearly show that the biofidelity of Hybrid dummies is not ensured during injuring tests and confirmed the observation made by Shaw and al. [4]. Despite little difference has been observed between cadaver and dummy for the resultant pelvis and chest accelerations, differences are observed on the components. This difference is well observed for the pelvis: the longitudinal acceleration is lower for the PHMS than for the dummy and the opposite is observed for the vertical acceleration. An explanation is the greater rigidity of the dummy pelvis compared to a cadaver pelvis. In simplified terms, the displacement of the dummy is practically parallel to the seating even though the PMHS pelvis rotate around the Y-axis.
The activation of the load limiters (4kN or 6kN) of the shoulder belt has been well observed on the belt force recording. As found by Kallieris et al. [6], the activation of the 4kN limiting effect during cadaver tests occurred approximately 25ms after the start of the belt loading. The effect of the load limit of the shoulder belt has not been well observed on the pelvis behaviour since the shoulder and pelvis belts were separated. In this case the pelvis belt has her own influence on the dynamics of the pelvis and reduces the influence of the load-limiting system.
Differences due to the load limit have been particularly observed on the thoracic and head dynamics of the PMHS: accelerations lessened with the decreasing of the load limit of the shoulder belt. This decreasing of accelerations lead to lower value of HIC showing that the use of a load limiting system reduces the injury risk of the head. However, the effect of the load limiting system on the dummy head dynamics was found less obvious. One of the reasons could be the rigidity of the dummy neck that might filter the effect of the load-limiting system. This rigidity simulates the muscle tone of living human (without considering any reaction time) whereas there is no muscle tone in the case of PMHS. Since the dummy is generally calibrated on slow speed volunteer tests. The influence of the reaction time in case of high speed is not clear. Concerning the PMHS, we thought that the absence of muscle tone is not really a problem because the impact time is very short.

As is found in literature, the location of the rib fractures corresponded to the contact area of the shoulder belt [6], [7], [8] and no bone injuries were found on the cervical spine [8]. The effect of the load limiting system has been shown since clavicle and sternum were not fractured using the lower load limit. Moreover, the greater rotation around the shoulder belt observed for the higher shoulder belt load could explain the higher number of right rib fractures for this configuration. Yet, MAIS levels obtained are high whatever the load limit of the shoulder belt, since all tests induced a high AIS level for the thorax. Despite the use of a low deceleration of the sled (20g to 24g), included in the corridor of the R44-03 regulation, the impact appeared severe in terms of injuries of the rib cage and numerous rib fractures were obtained whatever the load limit. Considering the age of the subjects, our results in terms of thoracic injuries agree with the known injury risk curves established on the basis of sled tests conducted by the University of Heidelberg [6]. For the subjects aged 70, a 4kN shoulder load corresponds to a 100% probability of AIS>3.
These injury observations show the interest of the shoulder belt load as injury indicator, contrary to the chest acceleration measurements, which are difficult to analyse since the measurement direction change during the test. Yet, injury observations made after the test using the 6kN-load limit (many fractures observed on both sides of the rib cage) show that the load distribution along the belt is also important.

CONCLUSIONS

Two series, each comprising two cadavers and two Hybrid III dummy tests, were carried out at INRETS - LBMC. The first series used a seat equipped with a 6kN load-limited shoulder belt and the second used a 4kN load-limited belt.

As expected, results showed that the dummy biofidelity is not ensured in the case of injuring tests, and this test device does not allow a precise analysis of the injury levels and mechanisms. For that numerical models are considered, which would reproduce the human behaviour whatever the load levels. The basic assumption of the HUMOS project is that a biofidelic model shall be structurally very close to the real human body. This assumption means that a correct representation of the main human structures is needed, the skeleton, but also the main organs and muscles. A biomechanical knowledge is also needed in order to validate the model with a realistic behaviour in a car crash situation. The data obtained from the cadaver tests presented in this paper will be used as reference data for the validation of this numerical model of the human body.
Concerning the force-limited belt, it has been shown that the lower load-limit belt is more effective in reducing the occupant's injuries. This new safety device associated with an air bag reduces considerably the injury risk of the car occupant and is found in most recent cars. Considering this new restraint system, new data concerning the human behaviour will be necessary for the assessment of the biofidelity of dummies and numerical models. For that, further tests with an airbag will be performed and particular attention will be made regarding the chest, lumbar spine, thorax/shoulder complex and neck behaviours.

ACKNOWLEDGMENTS

The HUMOS project is supported by European Community (DG XII) and co-ordinated by LAB (Laboratory of Accidentology, Biomechanics and human behaviour) PSA Peugeot Citroën Renault. The partners involved in the HUMOS program are : PSA Peugeot-Citroën, Renault, Volvo, VW, BMW, ISAM GmbH, TNO Automotive, FAURECIA, Chalmers University, Heidelberg University, Marseille University of Medicine, National Technical University of Athens.
The authors would like to thank to the Doctor Eric Voiglïo (surgeon of the Hospital of Lyon) from the University of Medicine, Claude Bernard Lyon, and the Doctor Michelle Ramet from the INRETS-LBMC for their contributions to the PMHS experiments and the autopsy and the injury description.
The authors would like to thank Pierre Lapelerie, Michel Marais, Sophie Serindat, Gérard Goutelle, Marcel Callejon and Alain Gilibert, for doing such a good job in collecting data, photos, measurements, during the experiments.

REFERENCES

[1] K. Bruyere, F. Bermond, R.Bouquet, Y. Caire, M. Ramet, E. Voiglio, "Human Maxilla Bone Response to 30° Oriented Impacts and Comparison with Frontal Bone Impacts ", 44th Annual Scientific Conference of the AAAM, 1-4 October, Chicago, Illinois
[2] R.H. Eppinger, J.H. Marcus, R.M. Morgan, Development of Dummy and Injury Index for NHTSA's Thoracic Side Impact Protection Research Program, SAE Publication N° 840885, Government /Industry Meeting and Exposition, May 21-24, 1984, Washington, D.C.
[3] G. Faverjon, J.Y. Foret-Bruno, C. Got, Y. Morvan, M. Lepage, L. Portier, C. Thomas, H. Vallee, Abbreviated Injury Scale - 1990 Revision, abbreviated impairment scale - 1994 Revision French translation, June 1994
[4] G. Shaw, J. Crandall, J. Butcher, Biofidelity of the THOR advanced frontal crash test dummy, IRCOBI Conference, September 2000, Montpellier, France.
[5] A. King, D.C. Viano, N. Mizeres, J.D. States, Humanitarian benefits of cadaver research on injury prevention, The journal of Trauma : Injury, Infection and Critical Care, Vol. 38, No.4, pp 564-569, 1995.
[6] D. Kallieris, A. Rizzetti, R. Mattern, R. Morgan, R. Epppinger, L. Keenan, On the synergism of the driver air bag and the 3-point belt in frontal crashes, Proceedings of the 39th STAPP Car Crash Conference, N° 952700, pp 389-401, November 8-10, 1995, San Diego, California.
[7] G. Schmidt, D. Kallieris, J. Barz, R. Mattern, J. Klaiber, Neck and thorax tolerance levels of belt-protected occupants in head-on collisions, Proceedings of the 19th STAPP Car Crash Conference, N° 751149, pp 225-257, , November 17-20, 1975, San Diego, California.
[8] C. Got, J.Y. Foret-Bruno, X. Troseille, J.Y. Le Coz, F. Bendjellal, C. Steyer, T. Phalempin, D. Villeforceix, P. Dandres, Thoracic injury risk in car crashes with occupant restrained with belt load limiter. Proceedings of the 42nd STAPP Car Crash Conference, N° 983166, pp 331-352, November 2-4, 1998, Tempe, Arizona.